

Cross-Covariate Gait Recognition: A Benchmark

Shinan Zou¹, Chao Fan^{2,3}, Jianbo Xiong¹, Chuanfu Shen^{2,4}, Shiqi Yu^{2,3}, Jin Tang^{1*}

¹School of Automation, Central South University

²Department of Computer Science and Engineering, Southern University of Science and Technology

³Research Institute of Trustworthy Autonomous System, Southern University of Science and Technology

⁴The University of Hong Kong

{zoushinan, jianbo_x, tjin}@csu.edu.cn, {12131100, 11950016}@mail.sustech.edu.cn, yusq@sustech.edu.cn

Abstract

Gait datasets are essential for gait research. However, this paper observes that present benchmarks, whether conventional constrained or emerging real-world datasets, fall short regarding covariate diversity. To bridge this gap, we undertake an arduous 20-month effort to collect a cross-covariate gait recognition (CCGR) dataset. The CCGR dataset has 970 subjects and about 1.6 million sequences; almost every subject has 33 views and 53 different covariates. Compared to existing datasets, CCGR has both population and individual-level diversity. In addition, the views and covariates are well labeled, enabling the analysis of the effects of different factors. CCGR provides multiple types of gait data, including RGB, parsing, silhouette, and pose, offering researchers a comprehensive resource for exploration. In order to delve deeper into addressing cross-covariate gait recognition, we propose parsing-based gait recognition (ParsingGait) by utilizing the newly proposed parsing data. We have conducted extensive experiments. Our main results show: 1) Cross-covariate emerges as a pivotal challenge for practical applications of gait recognition. 2) ParsingGait demonstrates remarkable potential for further advancement. 3) Alarming, existing SOTA methods achieve less than 43% accuracy on the CCGR, highlighting the urgency of exploring cross-covariate gait recognition. Link: <https://github.com/ShinanZou/CCGR>.

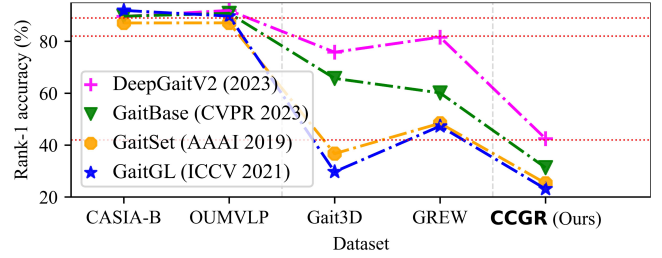
Introduction

Gait recognition aims to use physiological and behavioral characteristics extracted from walking videos to certify individuals' identities. Compared to other biometric modalities, such as face, fingerprints, and iris, gait patterns have the distinct advantage of being extracted from a distance in uncontrolled environments. These strengths place gait recognition as an effective solution for security applications.

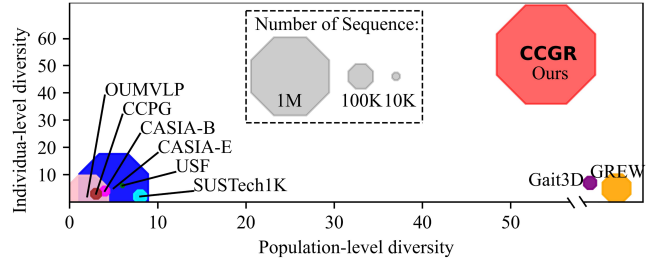
In the latest literature, the research on gait recognition is developing rapidly, with the evaluation benchmark developing from early indoor to outdoor environments. During this remarkable journey, most representative gait models (Chao et al. 2019; Lin, Zhang, and Yu 2021) boasting historical progress have unexpectedly performed unsatisfactory results when faced with emerging challenges posed by real-world gait datasets such as GREW (Zhu et al. 2021)

*Corresponding Author

Copyright © 2024, Association for the Advancement of Artificial Intelligence (www.aaai.org). All rights reserved.



(a). Performance differences of SOTA methods on commonly used datasets.



(b). Covariate diversity and the number of sequences.

Figure 1: Differences between CCGR and other datasets. Population-level diversity is roughly quantified by the count of covariate categories present within the whole dataset. Correspondingly, individual-level diversity is measured by the count of covariate categories for each subject. Here, the population-level diversity of Gait3D and GREW is rich, but the exact amount is unknown due to the wild scenarios.

and Gait3D (Zheng et al. 2022). Surprisingly, successive works (Fan et al. 2023b,a) quickly address this performance gap to a large extent, rekindling the promise of gait recognition for practical applications, as illustrated in Figure 1(a). However, this paper argues that the gait recognition task is much more challenging than these datasets have defined.

In general, previous indoor gait datasets often require subjects repeatedly walk along fixed paths while introducing variations in clothing and carrying. This approach yields controllable and well-annotated data, facilitating the early exploration of key covariates influencing recognition accuracy. However, as shown in Fig. 1(b), these datasets fall short regarding **population-level diversity**, as subjects of them contain the same limited group of covariates. Conversely,

Table 1: Comparison of CCGR with existing datasets. Sil., Inf., A., and 3DM. mean silhouette, infrared, audio, and 3D Mesh&SMPL. #Id, #Seq, and #Cam refer to the number of identities, sequences, and cameras. BAC, CO, GR, BR, DU, IN, BA, TR, SH, CL, UB, OC, NI, and WS are abbreviations of backpack, concrete, grass, briefcase, duration, incline, ball, treadmill, shoes, clothing, umbrella, uniform, occlusion, night and walking style. CMU MoBo (Gross and Shi 2001); SOTON (Shutler et al. 2004); USF (Sarkar et al. 2005); CASIA-B (Yu, Tan, and Tan 2006); CASIA-C (Tan et al. 2006); OU-ISIR Speed (Mansur et al. 2014); OU-ISIR Cloth (Altab Hossain et al. 2010); OU-ISIR MV (Makihara, Mannami, and Yagi 2011); OU-LP (Iwama et al. 2012); TUM GAID (Hofmann et al. 2014); OU-LP Age (Xu et al. 2017); OU-MVLP (Takemura et al. 2018; An et al. 2020; Li et al. 2022); OU-LP Bag (Uddin et al. 2018); GREW (Zhu et al. 2021); ReSGait (Mu et al. 2021); UAV-Gait (Ding et al. 2022); Gait3D (Zheng et al. 2022); CASIA-E (Song et al. 2022); CCPG (Li et al. 2023); SUSTech1K (Shen et al. 2023).

Dataset	#Id	#Seq	#Cam	Data types	Covariates except view	Environment	Diversity
CMU MoBo	25	600	6	RGB, Sil.	TR, Speed, BA, IN	Controlled	Not Rich
SOTON	115	2,128	2	RGB, Sil.	TR	Controlled	Not Rich
USF	122	1,870	2	RGB	CO, GR, SH, BR, DU	Controlled	Not Rich
CASIA-B	124	13,640	11	RGB, Sil.	Coat, Bag	Controlled	Not Rich
CASIA-C	153	1,530	1	Inf., Sil.	SP, Bag	Controlled	Not Rich
OU-ISIR Speed	34	612	1	Sil.	TR, Speed	Controlled	Not Rich
OU-ISIR Cloth	68	2,764	1	Sil.	TR, CL	Controlled	Not Rich
OU-ISIR MV	168	4,200	25	Sil.	TR	Controlled	Not Rich
OU-LP	4,007	7,842	2	Sil.	None	Controlled	Not Rich
TUM GAID	305	3,370	1	RGB, Depth, A.	DU, BAC, SH	Controlled	Not Rich
OU-LP Age	63,846	63,846	1	Sil.	Age	Controlled	Not Rich
OU-MVLP	10,307	288,596	14	Sil., Pose, 3DM.	None	Controlled	Not Rich
OU-LP Bag	62,528	187,584	1	Sil.	Carrying	Controlled	Not Rich
GREW	26,345	128,671	882	Sil., Flow, Pose	Free walking	Wild	Population-Level
ReSGait	172	870	1	Sil., Pose	Free walking	Wild	Population-Level
UAV-Gait	202	9,895	6	Sil., pose	None	Controlled	Not Rich
Gait3D	4,000	25,309	39	Sil., Pose, 3DM.	Free walking	Wild	Population-Level
CASIA-E	1,014	778,752	26	RGB, Sil.	Bag, CL, WS	Controlled	Not Rich
CCPG	200	16,566	10	RGB, Sil.	CL	Controlled	Not Rich
SUSTech1K	1,050	25,279	12	RGB, Sil., 3DP	Bag, CL, UB, OC, NI	Controlled	Not Rich
CCGR (ours)	970	1,580,617	33	RGB, Parsing, Sil., Pose	53 types per subject, as detailed in Figure 2.	Controlled	Population- and Individual-Level

the emergence of outdoor datasets effectively addresses this limitation due to their real-world collection scenarios. Although their data distribution closely mirrors practical applications, we contend that current outdoor gait datasets lack **individual-level diversity**, as each subject typically contributes no more than seven variants (sequences) on average. This situation gives rise to two potential drawbacks for research: a) A majority of data pairs may qualify as “easy cases” owing to limited collection areas and short-term data gathering. b) The lack of fine annotations blocks exploring critical challenges relevant to real-world applications. More details of the existing dataset are in Table 1.

To overcome these limitations, we propose a novel gait recognition benchmark that introduces both population-level and individual-level diversity, named **Cross-Covariate Gait Recognition** or **CCGR**. Statistically, the CCGR dataset covers 970 subjects and approximately 1.6 million walking sequences. These sequences span 53 distinct walking conditions and 33 different filming views. Thus, each subject within CCGR ideally contains a comprehensive collection of $53 \times 33 = 1,749$ sequences. Notably, the walking conditions are widely distributed and well annotated, encompassing diverse factors such as carried items (book, bag, box, umbrella, trolley case, heavy bag, and heavy box), road types (up the stair, down the stair, up the ramp, down the ramp, bumpy road, soft road, and curved road), styles of walking

(fast, stationary, normal, hands in pockets, free, and crowd), and more. The all-side camera array consisting of 33 cameras is installed at five different heights, effectively simulating the pitching angles of typical CCTVs. Every subject is recruited through a transparent process and accompanied by written consent. The age range of subjects spans from 6 to 70 years. The dataset encompasses raw RGB sequences. Releasing RGB images can facilitate the exploration of camera-based gait representations, and this paper officially provides common gait data like silhouette, parsing, and pose. CCGR will be made publicly available for research purposes.

Equipped with the proposed CCGR, we re-implement several representative state-of-the-art methods and investigate that: 1) Cross-covariate gait recognition is more challenging than that simulated by previous gait datasets, as the achieved best rank-1 accuracy is only 42.5%. 2) Certain less-researched covariates, such as the crowd, umbrella, overhead view, walking speed, road, mixed covariate, and more, significantly degrade the recognition accuracy. 3) The more covariates involved, regardless of population-level and individual-level diversity perspectives, the more challenging gait recognition becomes.

To solve complex covariate problems, this paper further introduces human parsing, which contains many semantic characteristics that describe body parts, to form a parsing-based baseline framework termed **ParsingGait**. In practice,

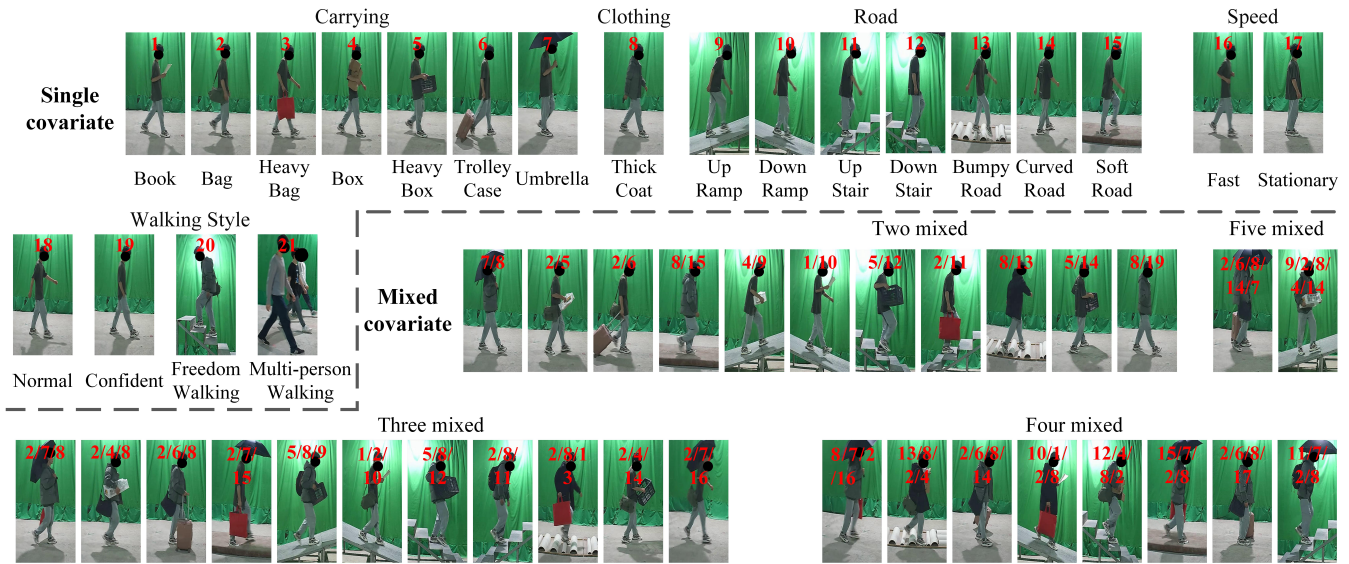


Figure 2: Examples of 53 covariates in CCGR. For a single covariate (the 1st row and the left of the 2nd row), the red numbers at the top of the pictures are indices of the covariates. For mixed covariates, numbers separated by “/” at the top of the picture indicate the co-occur of multi-single covariates corresponding to these numbers.

we instantiate the backbone of PrasingGait using various silhouette-based gait models, consistently achieving significant enhancements. By this means, this paper highlights the value of informative gait representations like human parsing images for gait pattern description.

In summary, our main contributions are as follows:

- We present the first well-annotated million-sequence-level gait recognition benchmark called CCGR, designed to research cross-covariate gait recognition deeply.
- We propose an efficient, compatible, and feasible parsing-based baseline framework named ParsingGait.
- We begin by evaluating existing algorithms to establish a baseline, then validating the effectiveness of ParsingGait. Next, we demonstrate the necessity of incorporating both population- and individual-level diversity. Finally, we thoroughly explore the impact of covariates and views.

The CCGR Benchmark

Covariates of CCGR

The dataset has 53 covariates; 21 are single covariates, while the remaining 32 are mixed covariates. Examples of the 53 covariates are shown in Figure 2.

Carrying: We have defined seven carrying covariates: **book**, **bag**, **heavy bag**, **box**, **heavy box**, and **trolley case**, **umbrella**. We have prepared 12 different types for the bag category, including single-shoulder bags, double-shoulder bags, satchels, backpacks, and handbags. Similarly, we have prepared eight boxes with varying shapes and volumes for the box category. As for the trolley case, we have prepared options in both 20-inch and 28-inch sizes. When subjects are asked to carry a bag, box, or trolley case, they can choose from the props we have provided. In the case of the heavy bag and box, we have placed counterweights inside them,

ranging from 8kg to 15kg, to simulate the desired weight.

Clothing: Regarding the **thick coat** covariates, we have prepared a selection of 20 clothing items, which include down coats, overcoats, windbreakers, jackets, and cotton coats. When subjects are instructed to wear a thick coat, they can choose from our clothing collection.

Road: In addition to the normal road, we have prepared seven road covariates: **up/down the stair**, **up/down the ramp**, **bumpy road**, **soft (muddy) road**, and **curved road**. Ramps have a slope of 15° . Curved road means subjects are asked to walk a curved track instead of a straight path.

Speed: In addition to the normal walking speed, we discuss two additional walking speeds: **fast** and **stationary**. Fast entails the subject walking at a speed close to a trot, while stationary refers to the subject remaining unmoving.

Walking Style: The remaining four single covariates include **normal walking**, **confident**, **multi-person walking**, and **freedom walking**. Normal walking indicates walking on a horizontal path at a normal speed without wearing a thick coat or carrying any items. Confident means that subjects place their hands inside their pant or clothing pockets. Multi-person walking means multiple subjects walking together. Freedom walking means subjects are free to choose their carrying, clothing, road, and speed.

Mixed covariates: In the real world, multiple covariates often co-occur. For instance, a man may wear a thick coat, carry a bag, and walk up a ramp. To simplify matters, we utilize mixed covariates to represent the co-occurrence of multiple covariates. In CCGR, we have designed 32 **mixed covariates** that are frequently encountered in daily life. Refer to Figure 2 for further details about these mixed covariates.



Figure 3: Examples of 33 views in CCGR. The red numbers at the top of the picture represent the horizontal angle.

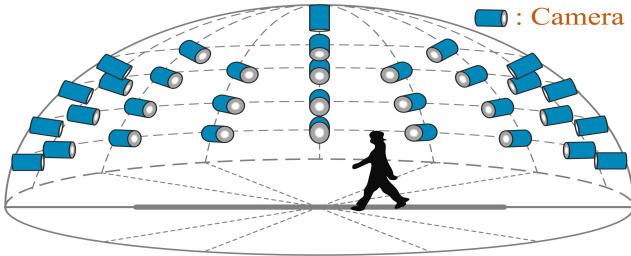


Figure 4: Camera setup in CCGR.

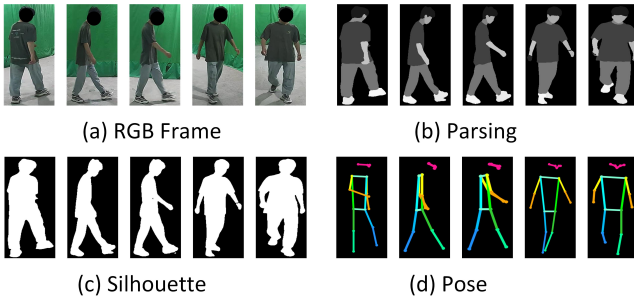


Figure 5: Examples of different gait data in CCGR .

Views of CCGR

We rent a 500-square-meter warehouse and set up 33 cameras to collect data. Camera settings are shown in Figures 4. The cameras are divided into five layers, from bottom to top. Layer 5 is the overhead camera with a pitch angle of 90° . For the other four layers, the pitch angles from bottom to top are 5° , 30° , 55° , and 75° , and the horizontal angles of each layer increase from 0° to 180° counterclockwise. The frame size of the video files is 1280×720 , and the frame rate is 25 fps. Figure 3 shows the example with various views.

Extraction of Multiple Gait Data

We offer various types of gait data, including RGB, parsing, silhouette, and pose; examples can be seen in Figure 5.

Parsing: Predicting the semantic category of each pixel on the human body is a fundamental task in computer vision, often referred to as human parsing (Liang et al. 2018;

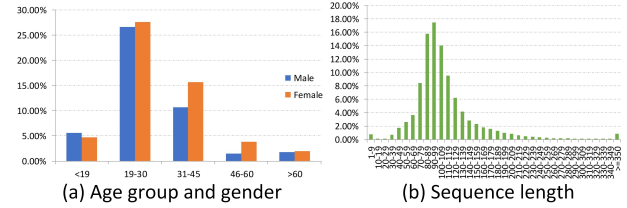


Figure 6: Age group, gender, and sequence length attributes. Ages are categorized into five groups (< 19 , $19-30$, $31-45$, $46-60$, and > 60). Sequence lengths are grouped at intervals of 10 frames, except for those greater than 350 frames.

Zhao et al. 2018; Gong et al. 2018; Xia et al. 2017). We uses QANet (Yang et al. 2021) for parsing extraction. QANet takes an RGB image as its input and produces the semantic category of each pixel on the human body, including hair, face, and left leg. Initially, QANet employed integers ranging from 0 to 19 to represent these different categories. To facilitate visualization and image pruning, we multiply these integers by 13 to generate a grayscale image.

Silhouette: We generate the silhouettes by directly binarizing the previously acquired parsing images. We have also tried the instance and semantic segmentation algorithms but attained relatively inferior gait recognition accuracy.

Pose: We use HRNet (Sun et al. 2019) to extract 2D Pose. We also try AlphaPose (Fang et al. 2017) and Openpose (Cao et al. 2017), which result in inferior accuracy.

Collection, Statistics and Evaluation

Collection Process: To simplify the description, we refer to covariates mentioned in the previous subsection as the “walking conditions”. In the normal walking condition, each subject walks twice. In the remaining 52 walking conditions, each subject only walks once per condition. Therefore, a total of 54 walks per subject are required. Since each subject has to walk 54 times, and the walking conditions have to be changed each time, it takes 2 hours to collect one subject.

Dataset statistics: Figure 6 presents the distribution of age, gender, and sequence length in CCGR. The proportions of the various covariates align with the number of walks for each covariate. Furthermore, CCGR exhibits an average of

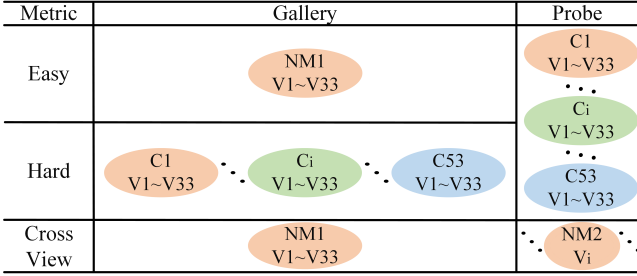


Figure 7: Evaluation metrics. C and V denote covariates and views, where subscripts indicate the order. NM is normal walking. “Easy” is employed by CASIA-B and OUMVLP (the gallery is normal walking). “Hard” is similar to GREW and Gait3D, closer to real life (the gallery is uncertain). The cross-view setting inherits from OU-MVLP.

110 frames per sequence.

Evaluation Protocol: Subjects are labeled from 1 to 1000. Subjects 134 to 164 are missing. Subjects 1 to 600 are used for training, and the rest are used for testing. The evaluation metrics are illustrated in Figure 7.

Parsing-based Gait Recognition

Although silhouette and pose are commonly employed as gait modalities, they possess significant limitations. Silhouette provides only contour information, while pose offers solely structural details, resulting in sparse and simplistic representations. Consequently, these modalities prove less effective when confronted with complex covariate environments. We are fortunate to discover that parsing can simultaneously provide contour, structural and semantic information. Notably, parsing eliminates texture and color, providing a basis for treating as a gait pattern.

Parsing and silhouettes have similar data structures, enabling parsing to inherit all silhouette-based algorithms without modification. This convenient compatibility allows us to explore parsing-based gait recognition efficiently. This paper explores the effectiveness of “Parsing + silhouette-based algorithms” and calls it **ParsingGait**.

Baseline on CCGR

Appearance-based Approaches

GEINet (Shiraga et al. 2016) adopts a four-layer CNN to learn gait features from GEIs. GaitSet (Chao et al. 2019) proposes to consider the gait as a set. GaitPart (Fan et al. 2020) focuses on fine-grained feature extraction and micro-motion feature capture in different body parts. CSTL (Huang et al. 2021) proposes a temporal modeling module to fuse multi-scale temporal features. GaitGL (Lin, Zhang, and Yu 2021) designs local and global 3D CNNs to extract gait’s local and global spatial features. GaitBase (Fan et al. 2023b) provides a structurally simple, empirically powerful, and practically robust baseline model, GaitBase. DeepGaitV2 (Fan et al. 2023a) provides a 22-layer network to address the entire outdoor dataset with many covariates.

Table 2: The accuracy of representative methods on CCGR.

Methods	Year	$R-1^{hard}$	$R-1^{easy}$	$R-5^{easy}$	$R-5^{hard}$
GEINet	2016	3.10	4.62	9.20	12.7
GaitSet	2019	25.3	35.3	46.7	58.9
GaitPart	2020	22.6	32.7	42.9	55.5
GaitGL	2021	23.1	35.2	39.9	54.1
CSTL	2021	7.25	11.8	13.79	20.1
GaitBase	2023	31.3	43.8	51.3	64.4
DeepGaitV2	2023	42.5	55.2	63.2	75.2
GaitGraph	2021	15.2	25.2	37.2	51.6
GaitGraph2	2022	0.26	0.27	1.4	1.41

Table 3: The accuracy of ParsingGait on CCGR.

Methods	Backbone	$R-1^{hard}$	$R-1^{easy}$	$R-5^{easy}$	$R-5^{hard}$
Parsing Gait (Ours)	GaitSet	31.6	42.8	54.8	67
	GaitPart	29.0	40.9	51.5	64.5
	GaitGL	28.4	42.1	46.6	61.4
	CSTL	27.9	40.7	47.1	61.5
	GaitBase	43.2	56.9	63.7	76.0
	DeepGaitV2	52.7	67.2	74.7	87.7

Implementation details: All silhouettes are aligned by the approach mentioned in (Takemura et al. 2018) and transformed to 64×44 . The batch size is $8 \times 16 \times 30$, where 8 denotes the number of subjects, 16 denotes the number of training samples per subject, and 30 is the number of frames. The optimizer is Adam. The number of iterations is 320K. The learning rate starts at $1e-4$ and drops to $1e-5$ after 200K iterations. For GaitBase and DeepGaitV2: The optimizer is SGD. The number of iterations is 240K. The learning rate starts at $1e-1$ and drops by $1/10$ at 100k, 140k, and 170k. All models are trained on the entire training set; this enables the model to be trained well in some experiments, and in general, with less than 5000 sequences, it is simply impossible to train a larger model well.

Model-based Approaches

GaitGraph (Teepe et al. 2021) treats the human skeleton as a graph and then extracts the structural features using a graph convolutional neural network. We train it for 1200 epochs with a batch size of 128. GaitGraph2 (Teepe et al. 2022) proposes a multi-branch graph-based interpretation of gait together with a GCN architecture. We train it for 500 epochs with a batch size of 768.

Experiment

Analysis of Representative Methods

The results are shown in Table 2. The $R-1^{hard}$ of GEINet, GaitSet, GaitPart, GaitGL, and CSTL falls below 26%. While these methods demonstrate near 90% accuracy on previous indoor datasets, their validity under complex covariates remains untested. In addition, GaitGraph and GaitGraph2 exhibit poorer performance than silhouette-based methods because the pose is sparser than silhouette.

GaitBase and DeepGaitV2 are proposed to address the challenge of outdoor datasets; they are more robust against

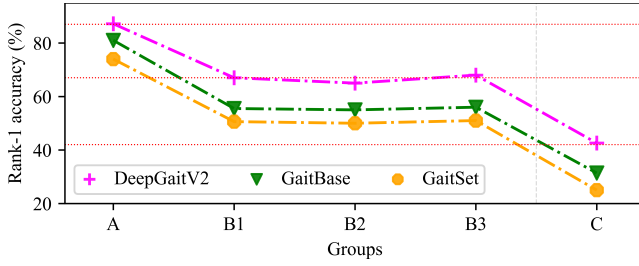


Figure 8: Impact of population and individual diversity.

Table 4: **Covariate Sampling Setup.** Seq, Sbj, and NoC refer to the sequence, subject, and number of covariates.

Groups	Similar to	Sample Setup	NoC per Sbj	NoC of the Sub-dataset
A	CASIA-B	NM, BG, CL, Layer1	3	3
B1	Gait3D/ GREW	random 8 Seqs per Sbj	Max 8	53
B2		random 8 Seqs per Sbj	Max 8	53
B3		random 8 Seqs per Sbj	Max 8	53
C	Ours	Use all sequences	53	53

complex covariates. However, **DeepGaitV2 achieves an impressive 82% rank-1 accuracy on the outdoor dataset GREW. In contrast, its performance on CCGR falls considerably below, reaching a mere 43%.** This disparity may be due to the lack of individual-level diversity in the existing outdoor datasets.

Analysis of Parsing-based Gait Recognition

As shown in Table 3, the accuracy of ParsingGait is substantially improved. These findings effectively illustrate the three main advantages of parsing: feasibility, validity, and compatibility. By distinguishing between different body parts, parsing makes it more robust in the face of complex covariates. ParsingGait is the same computationally efficient as its silhouette-based counterpart because our parsing is consistent with the silhouette data structure.

Population and Individual-Level Diversity

We research the impact of covariate diversity by sampling and isolating various covariates. The specific sampling setup is provided in Table 4. The experiments are categorized into five groups. Group A represents the absence of covariate diversity, while Group B demonstrates population-level diversity without individual-level diversity. Lastly, Group C exhibits both population-level and individual-level diversity. To simulate the short-term collectio, Group B is sampled in 2 specific ways: 1) One covariate per ID is randomly sampled, and then eight views under that covariate were randomly sampled. 2) One view per ID is randomly sampled, and then eight covariates under that view are randomly sampled. During the operation, two ways are randomly selected.

Based on the experimental data in Figure 8. From A to B1/2/3, the accuracy averagely decreased by -18.6%. However, from B1/2/3 to C, the accuracy averagely decreased by -25.1%. These findings indicate that **relying solely on population-level diversity is insufficient to accurately**

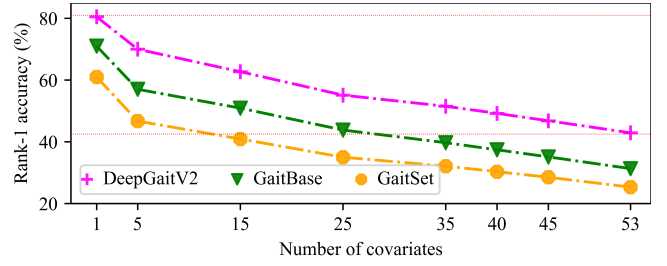


Figure 9: Impact of the number of covariates.

represent the underlying challenge, while individual-level diversity also is a significant challenge. In addition, the trend of Figure 8 is generally consistent with Figure 1 at the beginning of the paper, further strengthening the credibility of the experimental results.

Impact of the Number of Covariates

We examine how the number of covariates impacts accuracy, and the experimental outcomes are illustrated in Figure 9. The accuracy is substantially decreased as we progressively increase the covariate number from 1 to 53. Furthermore, a troubling trend emerges: even when the number reaches 53, the decline in accuracy rate does not significantly decelerate. This observation may indicate that gait recognition faces greater challenges in real-world scenarios, hinting at potential obstacles in open-world conditions.

Table 5: **Single-Covariate Evaluation:** R-1^{easy} accuracy (%) with excluding identical-view cases. ↓ and **bold** respectively indicate the sub-Average and SOTA performance.

Gallery: Normal 1					
Publication			CVPR23	Arxiv23	Ours
Type	Covariate	Abbr.	GaitBase	DeepGaitV2	ParsingGait
Carrying	Book	BK	65.7	75.3	85.5
	Bag	BG	64.9	75.4	86.1
	Heavy Bag	HVBG	60.0↓	72.3	84.2
	Box	BX	61.5	71.6	83.0
	Heavy Box	HVBX	58.7↓	69.7↓	81.9↓
	Trolley Case	TC	64.1	73.0	83.4
	Umbrella	UB	47.2↓	60.5↓	71.3↓
	<i>Average</i>	-	60.3	71.1	82.2
Clothing	Thick Coat	CL	40.4	53.5	66.8
Road	Up Ramp	UTR	60.3↓	69.5↓	80.9
	Down Ramp	DTR	60.5↓	70.1↓	80.2
	Up Stair	UTS	54.9↓	66.7↓	78.0↓
	Down Stair	DTS	54.0↓	65.4↓	76.7↓
	Bumpy Road	BM	63.3	71.4	82.0
	Curved Road	CV	70.0	77.3	86.1
	Soft Road	SF	66.0	73.2	83.7
	<i>Average</i>	-	61.3	70.5	79.3
Speed	Normal 1	NM1	76.6	83.5	91.3
	Fast	FA	47.2↓	60.7↓	74.1↓
	Stationary	ST	32.0↓	45.0↓	60.9↓
	<i>Average</i>	-	51.9	63.1	75.4
Walking Style	Normal 2	NM2	75.3	82.3	90.7
	Confident	CF	64.9	74.8	83.9
	Freedom	FD	57.1	68.1	79.2
	Multi-person	MP	24.0↓	32.6↓	39.4↓
	<i>Average</i>	-	55.3	64.4	73.3

Table 6: **Mixed-Covariate Evaluation:** R-1^{easy} accuracy (%) with excluding identical-view cases. We use “-” to connect the mixed covariates. Tab. 5 presents the dictionary containing abbreviations and their corresponding full spellings of these covariates. ↓ and **bold** respectively indicate the sub-Average and SOTA performance.

Gallery: Normal 1					
Publication		CVPR23	Arxiv23	Ours	
Category	Covariate	GaitBase	DeepGaitV2	ParsingGait	
Two Mixed	CL-UB	25.2↓	37.8↓	46.9↓	
	HVBX-BG	52.1	64.7	78.3	
	BG-TC	58.1	69.3	81.3	
	SF-CL	36.1↓	48.0↓	62.8↓	
	UTR-BX	51.0	62.0	75.4	
	DTR-BK	55.1	66.0	77.4	
	DTS-HVBX	42.6↓	56.1↓	69.8↓	
	UTS-BG	46.8	60.9	74.5	
	BM-CL	35.2↓	46.3	61.8	
	CV-HVBX	61.0	70.8	82.0	
	CL-CF	39.2↓	52.7↓	65.6↓	
	<i>Average</i>		45.7	57.7	70.5
Three Mixed	CL-UB-BG	23.4↓	36.1↓	44.9↓	
	BX-BG-CL	35.1↓	48.8	60.7	
	BG-TC-CL	34.3↓	48.5	63.0	
	SF-UB-BG	36.4↓	49.4	62.5	
	UTR-HVBX-CL	31.8↓	43.1↓	55.3↓	
	DTR-BK-BG	49.2	61.7	74.9	
	DTS-HVBX-CL	26.4↓	38.0↓	49.1↓	
	UTS-BG-CL	25.1↓	37.7↓	52.5↓	
	BM-CL-BG	33.0↓	44.8↓	59.6↓	
	CV-BX-BG	58.8	69.6	80.8	
	UB-BG-FA	28.0↓	41.0↓	52.8↓	
	<i>Average</i>		34.7	47.1	59.7
Four Mixed	CL-UB-BG-FA	16.2↓	27.6↓	35.7↓	
	BM-CL-BG-BX	32.2	43.5	56.1	
	BG-TC-CL-CV	38.0	51.2	66.9	
	DTR-BK-BG-CL	32.2	44.9	56.9	
	DTS-BX-CL-BG	25.6	37.3	48.9	
	SF-UB-BG-CL	20.6↓	31.8↓	41.9↓	
	BG-TC-CL-ST	11.7↓	18.4↓	29.4↓	
	UTS-UB-BG-CL	15.8↓	26.1↓	36.4↓	
	<i>Average</i>		24.0	35.1	46.5
	Five Mixed	BG-TC-CL-CV-UB	34.1	35.9	47.4
UTR-BG-CL-BX-CV		31.3	45.2	58.3	

Evaluation of Covariates and Views

In Table 2 and 3, we evaluate the overall performance of CCGR. Next, we analyze the impact of different covariates and views using the “easy” evaluation criteria. Covariates in Table 5 and 6 that are challenging and prone to causing failure have been denoted with ↓.

Single-Covariate Evaluation: As shown in Table 5. Multi-person walking significantly affects accuracy because many parts of the human body are obscured. Speed also significantly affects the accuracy as it dramatically impacts the temporal feature extraction of the algorithm. Clothing is still a big challenge. In addition, carrying and road also have a notable negative impact on accuracy.

Mixed-Covariate Evaluation: As shown in Table 6. Mixed covariates impact precision more, with a significant

Table 7: **Cross-View Evaluation:** Rank-1 accuracy (%) with excluding identical-view cases.

Cross-view Evaluation				
Publications		CVPR23	Arxiv23	Ours
Pitch Angle	Probe View	GaitBase	DeepGaitV2	ParsingGait
5°	0.0°	80.1	85.7	90.6
	22.5°	84.7	89.5	93.1
	45.0°	83.7	89.1	93.9
	67.5°	79.3	85.7	93.6
	90.0°	75.7	83.7	93.2
	112.5°	76.9	84.6	93.2
	135.0°	81.6	87.1	93.7
	157.5°	83.8	88.6	92.7
	180.0°	77.4	83.3	89.9
	<i>Average</i>		80.4	86.4
30°	0.0°	79.6	85.2	92.0
	22.5°	85.0	89.8	93.6
	45.0°	86.0	90.9	94.9
	67.5°	82.7	88.8	95.0
	90.0°	78.9	86.4	94.6
	112.5°	79.1	86.3	94.5
	135.0°	82.8	88.5	94.5
	157.5°	84.1	89.9	93.7
	180.0°	79.5	85.3	91.8
<i>Average</i>		82.0	87.9	93.9
55°	0.0°	74.8	81.8	90.6
	22.5°	81.5	86.7	93.3
	45.0°	83.9	88.9	95.0
	67.5°	82.2	88.4	95.1
	90.0°	63.6	76.3	92.0
	112.5°	77.3	84.5	93.6
	135.0°	81.2	87.4	93.9
	157.5°	80.8	86.3	93.2
	180.0°	75.9	83.2	91.3
<i>Average</i>		77.9	84.8	93.1
75°	0.0°	64.4	74.8	86.0
	45.0°	78.7	85.2	92.7
	90.0°	40.8	60.9	87.5
	135.0°	73.2	80.5	90.6
	180.0°	62.5	74.0	86.2
<i>Average</i>		63.9	75.1	88.6
OverHead	-	2.0	8.4	32.0

classical decrease as the number of mixes increases. for example, “Bag → BG-TC → BG-TC-CL → BG-TC-CL-ST”, accuracy is gradually declining. However, mixed covariates are a challenge that must be addressed because ideal conditions for single covariates in real life tend to be rare.

Cross-View Evaluation: As shown in Table 7. The existing algorithms perform well, considering only the views. The current challenge with views is how to address the high-pitch angle case. Encouragingly, ParsingGait demonstrates distinct improvement in recognizing overhead views, indicating that addressing high-pitch angles is promising.

Conclusion

This paper introduces CCGR, a well-labeled dataset consisting of over one million sequences, which provides diversity at both the population and individual levels. Our experiments demonstrate that individual-level diversity is as challenging as population-level diversity. As gait recognition on many public gait datasets is close to saturation, our dataset CCGR introduces more challenges, specifically more covariates, into gait recognition. Future works can explore how gait recognition is affected by different covariates and how to design robust gait recognition.

Acknowledgements

This work was supported by the Natural Science Foundation of Hunan Province (No.2023JJ30697), the Changsha Natural Science Foundation (No.kq2208286) and the National Natural Science Foundation of China (No.61502537). This work was also supported in part by the National Key Research, and in part by Development Program of China under Grant (No.61976144) and the Shenzhen International Research Cooperation Project under Grant (No.GJHZ20220913142611021).

Additional

Ethical Statement

All subjects are openly recruited and participate voluntarily, and they need to read and acknowledge the collection protocol by signature and fingerprint. In return, we pay each subject a fee for data copyright.

Analysis of Silhouette Extraction

Earlier work (Yu, Tan, and Tan 2006) uses **background subtraction** (Wang et al. 2003) to obtain silhouettes, but background subtraction requires heuristic pre-processing and is unsuitable for large-scale practical use. Recently, **GREW** (Zhu et al. 2021) uses the instance segmentation (**Ins-Seg**) algorithm HTC (Chen et al. 2019) to obtain silhouettes, and **Gait3D** (Zheng et al. 2022) uses the semantic segmentation (**Sem-Seg**) algorithm HRNet-segmentation (Wang et al. 2019) to obtain silhouettes. There are also unused panoramic segmentation (**Pan-Seg**) methods. We compare instance, semantic, and panoramic segmentation, except for background subtraction, which requires heuristic processing. For the three types of methods, we choose 3 SOTA algorithms: HTC (Chen et al. 2019), Segformer (Xie et al. 2021), and PanopticFPN (Kirillov et al. 2019).

Next, works (Liu et al. 2004; Choi, Napoleon, and van Gemert 2021) use the obtained parsing maps to improve the original silhouette, but their improved approach has heuristic processing, which may be less robust in complex environments. Work (Liu et al. 2004) uses manual parsing and is unusable on a large scale. We compare the improved silhouette (**Imp-s**) of work (Choi, Napoleon, and van Gemert 2021). The above works do not propose using the parsing directly as gait data; they only improve the original silhouette.

To save time, we conduct experiments on the CCGR-Mini (Subjects 1 to 60 are used for training, and subjects 961 to

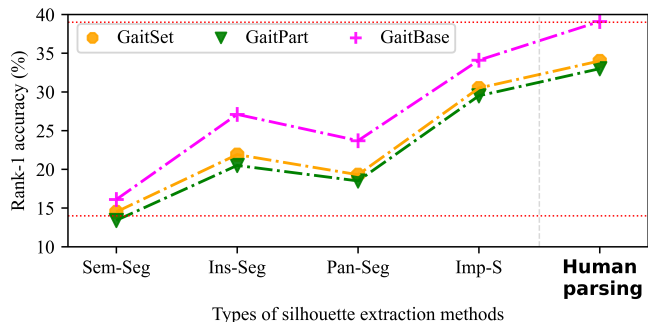


Figure 10: Rank-1 accuracy (%) on the CCGR-Mini when using different types of silhouette extraction methods. Sem-Seg, Ins-Seg, Pan-Seg, and Imp-s mean semantic segmentation, instance segmentation, panoramic segmentation, and improved silhouette.

100 are used for testing); this is sufficient for the comparison. The results are listed in figure 10.

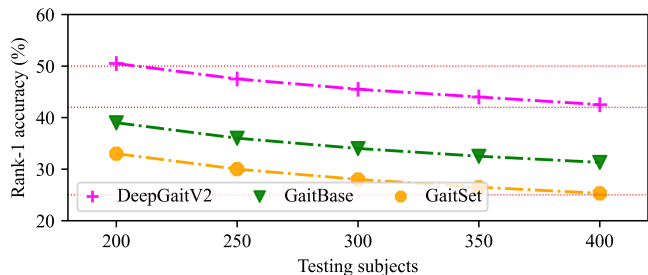


Figure 11: Rank-1 accuracy (%) with different numbers of testing subjects.

There is a significant improvement in accuracy when using human parsing. However, recognition accuracy is lower when using HTC, Segformer, and PanopticFPN because they are not initially designed for human segmentation. Improved silhouette (Imp-S) performs poorly, suggesting that this method is not robust to covariates.

Using more accurate silhouettes for CCGR remains very challenging, illustrating that **the diversity of covariates at the population and individual level** is the main reason for the challenge of the CCGR.

Impact of the number of testing subjects

Figure 11 shows the accuracy as the testing subjects decrease from 400 to 200. There is a slight improvement in accuracy as the number of testing subjects decreases. However, even if the testing subjects are reduced to 200, the accuracy is still relatively low, illustrating that **the diversity of covariates at the population and individual level** is the main reason for the challenge of the CCGR.

Evaluation of Covariates with “Hard” Metric

In the main text, we evaluate the covariates using the “easy” metric, and here we give a further evaluation under the “hard” metric. The results for “Single-Covariate Evaluation”

Table 8: **Single-Covariate Evaluation:** $R-1^{hard}$ accuracy (%) with excluding identical-view cases. \downarrow and **bold** respectively indicate the sub-Average and state-of-the-art performance.

Hard Metric					
Publication			CVPR23	Arxiv23	Ours
Type	Covariate	Abbr.	GaitBase	DeepGaitV2	ParsingGait
Carrying	Book Bag	BK	42.0	53.6	65.9
	Heavy Bag	BG	41.0	52.7	65.3
	Box	HVBG	38.4 \downarrow	50.1 \downarrow	63.6
	Heavy Box	BX	40.9	51.9	64.3
	Trolley Case	HVBX	39.7	51.1	63.5
	Umbrella	TC	41.3	52.7	65.4
		UB	27.8 \downarrow	40.0 \downarrow	51.0 \downarrow
	Average	-	38.7	50.3	62.7
Clothing	Thick Coat	CL	32.1	44.3	56.5
Road	Up Ramp	UTR	39.7	50.7	63.2
	Down Ramp	DTR	39.2 \downarrow	50.6 \downarrow	61.9 \downarrow
	Up Stair	UTS	36.9 \downarrow	49.5 \downarrow	61.9 \downarrow
	Down Stair	DTS	36.5 \downarrow	48.5 \downarrow	60.9 \downarrow
	Bumpy Road	BM	41.3	53.3	65.3
	Curved Road	CV	46.2	58.5	70.1
	Soft Road	SF	42.5	53.7	65.6
	Average	-	39.3	51.1	63.2
Speed	Normal 1	NM1	43.9	55.2	66.9
	Fast	FA	32.8	42.9	55.2
	Stationary	ST	19.2 \downarrow	27.9 \downarrow	40.9 \downarrow
	Average	-	32.0	42.0	54.4
Walking Style	Normal 2	NM2	43.9	55.3	67.1
	Confident	CF	42.0	54.2	64.8
	Freedom	FD	38.1	50.3	63.0
	Multi-Person	MP	0.8 \downarrow	0.8 \downarrow	1.0 \downarrow
	Average	-	31.2	40.2	49.0

and "Mixed-Covariate Evaluation" are shown in Table 8 and Table 9, respectively.

Hard metrics are more difficult than easy metrics, so there is a decrease in accuracy, but the trend in the impact of covariates does not change. Multi-person walking, speed, clothing, carrying, and road significantly affect gait. In the speed type, stationary had the most significant impact; in the carrying type, umbrellas had the most significant impact; and in the road type, stairs had the most significant impact.

Mixed covariates are more complex than single covariates because they introduce multiple changes simultaneously. With two-mixed, three-mixed, four-mixed, and five-mixed, the precision has gradually decreased. However, this is one of the challenges that must be addressed because natural walks often have multiple covariates simultaneously.

References

Altah Hossain, M.; Makihara, Y.; Wang, J.; and Yagi, Y. 2010. Clothing-invariant gait identification using part-based clothing categorization and adaptive weight control. *PR*, 43(6): 2281–2291.

An, W.; Yu, S.; Makihara, Y.; Wu, X.; Xu, C.; Yu, Y.; Liao, R.; and Yagi, Y. 2020. Performance Evaluation of Model-based Gait on Multi-view Very Large Population Database with Pose Sequences. *IEEE Trans. on Biometrics, Behavior, and Identity Science*.

Table 9: **Mixed-Covariate Evaluation:** $R-1^{hard}$ accuracy (%) with excluding identical-view cases. We use "-" to connect the mixed covariates. Tab. 5 presents the dictionary containing abbreviations and their corresponding full spellings of these covariates. \downarrow and **bold** respectively indicate the sub-Average and state-of-the-art performance.

Hard Metric				
Publication		CVPR23	Arxiv23	Ours
Category	Covariate	GaitBase	DeepGaitV2	ParsingGait
Two Mixed	CL-UB	20.3 \downarrow	31.9 \downarrow	40.4 \downarrow
	HVBX-BG	36.4	47.9	60.5
	BG-TC	38.8	50.4	63.9
	SF-CL	30.4 \downarrow	41.6 \downarrow	53.8 \downarrow
	UTR-BX	36.4	47.5	60.2
	DTR-BK	37.8	49.1	60.8
	DTS-HVBX	31.7 \downarrow	43.7 \downarrow	56.5 \downarrow
	UTS-BG	32.0 \downarrow	44.5 \downarrow	58.4
	BM-CL	28.9 \downarrow	41.0 \downarrow	53.7 \downarrow
	CV-HVBX	42.6	54.9	67.3
	CL-CF	31.5 \downarrow	43.7 \downarrow	55.7 \downarrow
	Average	33.4	45.1	57.4
Three Mixed	CL-UB-BG	19.4 \downarrow	30.6 \downarrow	39.0 \downarrow
	BX-BG-CL	28.1	40.2	51.3
	BG-TC-CL	28.4	40.5	53.6
	SF-UB-BG	24.7 \downarrow	36.2 \downarrow	47.4 \downarrow
	UTR-HVBX-CL	27.2 \downarrow	38.3 \downarrow	49.5 \downarrow
	DTR-BK-BG	35.2	46.7	58.9
	DTS-HVBX-CL	23.4 \downarrow	34.4 \downarrow	44.9 \downarrow
	UTS-BG-CL	23.1 \downarrow	34.4 \downarrow	47.5 \downarrow
	BM-CL-BG	28.4	40.2	52.5
	CV-BX-BG	41.4	53.6	65.9
UB-BG-FA	20.9 \downarrow	30.3 \downarrow	40.5 \downarrow	
	Average	27.3	38.7	50.1
Four Mixed	CL-UB-BG-FA	15.9 \downarrow	24.7 \downarrow	32.0 \downarrow
	BM-CL-BG-BX	27.5	39.2	50.3
	BG-TC-CL-CV	31.6	44.2	57.9
	DTR-BK-BG-CL	27.3	38.6	49.7
	DTS-BX-CL-BG	23.2	34.4	45.1
	SF-UB-BG-CL	18.4 \downarrow	28.7 \downarrow	37.6 \downarrow
	BG-TC-CL-ST	10.9 \downarrow	16.5 \downarrow	25.7 \downarrow
UTS-UB-BG-CL	15.1 \downarrow	24.6 \downarrow	34.1 \downarrow	
	Average	21.2	31.4	41.5
Five Mixed	BG-TC-CL-CV-UB	20.1	31.5	41.2
	UTR-BG-CL-BX-CV	29.0	40.9	52.3

Cao, Z.; Simon, T.; Wei, S.-E.; and Sheikh, Y. 2017. Real-time Multi-Person 2D Pose Estimation Using Part Affinity Fields. In *CVPR*.

Chao, H.; He, Y.; Zhang, J.; and Feng, J. 2019. GaitSet: Regarding Gait as a Set for Cross-View Gait Recognition. In *AAAI*.

Chen, K.; Pang, J.; Wang, J.; Xiong, Y.; Li, X.; Sun, S.; Feng, W.; Liu, Z.; Shi, J.; Ouyang, W.; Loy, C. C.; and Lin, D. 2019. Hybrid task cascade for instance segmentation. In *CVPR*.

Choi, Y.; Napoleon, Y.; and van Gemert, J. C. 2021. The Arm-Swing is Discriminative in Video Gait Recognition for Athlete Re-Identification. In *ICIP*.

Ding, T.; Zhao, Q.; Liu, F.; Zhang, H.; and Peng, P. 2022. A

- Dataset and Method for Gait Recognition with Unmanned Aerial Vehicleless. In *ICME*.
- Fan, C.; Hou, S.; Huang, Y.; and Yu, S. 2023a. Exploring Deep Models for Practical Gait Recognition. *ArXiv*, abs/2303.03301.
- Fan, C.; Liang, J.; Shen, C.; Hou, S.; Huang, Y.; and Yu, S. 2023b. OpenGait: Revisiting Gait Recognition Towards Better Practicality. In *CVPR*, 9707–9716.
- Fan, C.; Peng, Y.; Cao, C.; Liu, X.; Hou, S.; Chi, J.; Huang, Y.; Li, Q.; and He, Z. 2020. GaitPart: Temporal Part-Based Model for Gait Recognition. In *CVPR*.
- Fang, H.-S.; Xie, S.; Tai, Y.-W.; and Lu, C. 2017. RMPE: Regional Multi-Person Pose Estimation. In *ICCV*.
- Gong, K.; Liang, X.; Li, Y.; Chen, Y.; Yang, M.; and Lin, L. 2018. Instance-Level Human Parsing via Part Grouping Network. In *ECCV*, 805–822. ISBN 978-3-030-01225-0.
- Gross, R.; and Shi, J. 2001. The CMU Motion of Body (MoBo) Database. *Monumenta Nipponica*.
- Hofmann, M.; Geiger, J.; Bachmann, S.; Schuller, B.; and Rigoll, G. 2014. The TUM Gait from Audio, Image and Depth (GAID) database: Multimodal recognition of subjects and traits. *JVCIR*, 25(1): 195–206.
- Huang, X.; Zhu, D.; Wang, H.; Wang, X.; Yang, B.; He, B.; Liu, W.; and Feng, B. 2021. Context-Sensitive Temporal Feature Learning for Gait Recognition. In *ICCV*, 12909–12918.
- Iwama, H.; Okumura, M.; Makihara, Y.; and Yagi, Y. 2012. The OU-ISIR Gait Database Comprising the Large Population Dataset and Performance Evaluation of Gait Recognition. *IEEE Trans. on Information Forensics and Security*, 7, Issue 5: 1511–1521.
- Kirillov, A.; Girshick, R.; He, K.; and Dollar, P. 2019. Panoptic Feature Pyramid Networks. In *CVPR*.
- Li, W.; Hou, S.; Zhang, C.; Cao, C.; Liu, X.; Huang, Y.; and Zhao, Y. 2023. An In-Depth Exploration of Person Re-Identification and Gait Recognition in Cloth-Changing Conditions. In *CVPR*, 13824–13833.
- Li, X.; Makihara, Y.; Xu, C.; and Yagi, Y. 2022. Multi-View Large Population Gait Database With Human Meshes and Its Performance Evaluation. *IEEE Transactions on Biometrics, Behavior, and Identity Science*, 4(2): 234–248.
- Liang, X.; Gong, K.; Shen, X.; and Lin, L. 2018. Look into Person: Joint Body Parsing & Pose Estimation Network and a New Benchmark. *IEEE TPAMI*.
- Lin, B.; Zhang, S.; and Yu, X. 2021. Gait Recognition via Effective Global-Local Feature Representation and Local Temporal Aggregation. In *ICCV*, 14648–14656.
- Liu, Z.; Malave, L.; Osuntogun, A.; Sudhakar, P.; and Sarkar, S. 2004. Toward understanding the limits of gait recognition. In *Biometric Technology for Human Identification*. SPIE.
- Makihara, Y.; Mannami, H.; and Yagi, Y. 2011. Gait Analysis of Gender and Age Using a Large-Scale Multi-view Gait Database. In Kimmel, R.; Klette, R.; and Sugimoto, A., eds., *ACCV*, 440–451. Berlin, Heidelberg: Springer Berlin Heidelberg. ISBN 978-3-642-19309-5.
- Mansur, A.; Makihara, Y.; Aqmar, R.; and Yagi, Y. 2014. Gait Recognition under Speed Transition. In *CVPR*.
- Mu, Z.; Castro, F. M.; Marín-Jiménez, M. J.; Guil, N.; ran Li, Y.; and Yu, S. 2021. ReSGait: The Real-Scene Gait Dataset. In *IJCB 2021*.
- Sarkar, S.; Phillips, P.; Liu, Z.; Vega, I.; Grother, P.; and Bowyer, K. 2005. The humanID gait challenge problem: data sets, performance, and analysis. *IEEE TPAMI*, 27(2): 162–177.
- Shen, C.; Fan, C.; Wu, W.; Wang, R.; Huang, G. Q.; and Yu, S. 2023. LidarGait: Benchmarking 3D Gait Recognition With Point Clouds. In *CVPR*, 1054–1063.
- Shiraga, K.; Makihara, Y.; Muramatsu, D.; Echigo, T.; and Yagi, Y. 2016. GEINet: View-invariant gait recognition using a convolutional neural network. In *ICB*, 1–8.
- Shutler, J. D.; Grant, M. G.; Nixon, M. S.; and Carter, J. N. 2004. On a large sequence-based human gaitdatabase. In *Applications and Science in Soft Computing*.
- Song, C.; Huang, Y.; Wang, W.; and Wang, L. 2022. CASIA-E: a large comprehensive dataset for gait recognition. *IEEE Transactions on Pattern Analysis and Machine Intelligence*, 45(3): 2801–2815.
- Sun, K.; Xiao, B.; Liu, D.; and Wang, J. 2019. Deep High-Resolution Representation Learning for Human Pose Estimation. In *CVPR*.
- Takemura, N.; Makihara, Y.; Muramatsu, D.; Echigo, T.; and Yagi, Y. 2018. Multi-view large population gait dataset and its performance evaluation for cross-view gait recognition. *IPSJ Transactions on Computer Vision and Applications*, 10.
- Tan, D.; Huang, K.; Yu, S.; and Tan, T. 2006. Efficient Night Gait Recognition Based on Template Matching. In *ICPR*, volume 3, 1000–1003.
- Teepe, T.; Gilg, J.; Herzog, F.; Hörmann, S.; and Rigoll, G. 2022. Towards a Deeper Understanding of Skeleton-Based Gait Recognition. In *CVPRW*.
- Teepe, T.; Khan, A.; Gilg, J.; Herzog, F.; Hörmann, S.; and Rigoll, G. 2021. Gaitgraph: Graph Convolutional Network for Skeleton-Based Gait Recognition. In *2021 IEEE International Conference on Image Processing (ICIP)*, 2314–2318.
- Uddin, M. Z.; Ngo, T. T.; Makihara, Y.; Takemura, N.; Li, X.; Muramatsu, D.; and Yagi, Y. 2018. The OU-ISIR Large Population Gait Database with real-life carried object and its performance evaluation. *IPSJ Transactions on Computer Vision and Applications*, 10(1): 5.
- Wang, J.; Sun, K.; Cheng, T.; Jiang, B.; Deng, C.; Zhao, Y.; Liu, D.; Mu, Y.; Tan, M.; Wang, X.; Liu, W.; and Xiao, B. 2019. Deep High-Resolution Representation Learning for Visual Recognition. *IEEE TPAMI*.
- Wang, L.; Tan, T.; Ning, H.; and Hu, W. 2003. Silhouette analysis-based gait recognition for human identification. *IEEE TPAMI*.
- Xia, F.; Wang, P.; Chen, X.; and Yuille, A. L. 2017. Joint Multi-Person Pose Estimation and Semantic Part Segmentation. In *CVPR*.

- Xie, E.; Wang, W.; Yu, Z.; Anandkumar, A.; Alvarez, J. M.; and Luo, P. 2021. SegFormer: Simple and Efficient Design for Semantic Segmentation with Transformers. In *Advances in Neural Information Processing Systems*.
- Xu, C.; Makihara, Y.; Ogi, G.; Li, X.; Yagi, Y.; and Lu, J. 2017. The OU-ISIR Gait Database Comprising the Large Population Dataset with Age and Performance Evaluation of Age Estimation. *IPSN Trans. on Computer Vision and Applications*, 9(24): 1–14.
- Yang, L.; Song, Q.; Wang, Z.; Liu, Z.; Xu, S.; and Li, Z. 2021. Quality-Aware Network for Human Parsing. In *arXiv preprint arXiv:2103.05997*.
- Yu, S.; Tan, D.; and Tan, T. 2006. A Framework for Evaluating the Effect of View Angle, Clothing and Carrying Condition on Gait Recognition. In *ICPR*, volume 4, 441–444.
- Zhao, J.; Li, J.; Cheng, Y.; Sim, T.; Yan, S.; and Feng, J. 2018. Understanding Humans in Crowded Scenes: Deep Nested Adversarial Learning and A New Benchmark for Multi-Human Parsing. In *ACM MM*, 792–800. ISBN 9781450356657.
- Zheng, J.; Liu, X.; Liu, W.; He, L.; Yan, C.; and Mei, T. 2022. Gait Recognition in the Wild With Dense 3D Representations and a Benchmark. In *CVPR*, 20228–20237.
- Zhu, Z.; Guo, X.; Yang, T.; Huang, J.; Deng, J.; Huang, G.; Du, D.; Lu, J.; and Zhou, J. 2021. Gait Recognition in the Wild: A Benchmark. In *ICCV*, 14789–14799.